Background to the MODIS Weekly Maximum-NDVI Composites for Canada South of 60°N

Canada's agriculturally important lands include lands that are currently used for agricultural purposes (e.g. croplands, rangeland, pastures) as well as those that show potential for future agricultural development (e.g. natural grasslands). However, because these lands generally cover large geographical extents, their assessment by conventional ground survey techniques are often time-consuming and costly (Asrar et al. 1986; Bakhtiari and Zoughi 1991; Tucker 1980; Weiser et al. 1986). Thus, other monitoring approaches must be utilized. One possible approach is the use of satellite remote sensing systems.

Remote sensing, through the unique combination of extensive spatial, spectral and frequent temporal data collection, can provide scientists and managers with a powerful monitoring tool at a variety of landscape scales. The mounting of sensors on earth-orbiting vehicles has increased not only our "spatial" reach (i.e. the distance from which we are able to monitor the earth) but also our "spectral" reach (i.e. our ability to gather information from non-visible wavelengths of the electromagnetic spectrum) (Tucker 1980). Remotely-sensed data collection has the potential to provide quantitative information on the amount, condition, and type of vegetation, provided that the effects of physical and physiological processes on the spectral characteristics of canopies are fully understood.

One of the greatest challenges in the remote sensing of agricultural systems has been the reliable estimation of biophysical variables – such as aboveground biomass, net primary productivity and yield – from satellite platforms. This is largely a consequence of the "mixed pixel" problem, where factors other than the presence and amount of green vegetation (e.g. senescent vegetation, soil, shadow) combine to form composite spectra (see Asner 1998; Asner et al. 1998; Fourty et al. 1996; Goel 1988; Myeni et al. 1989; Ross 1981). Spectral mixing often makes the discrimination of green vegetation difficult and has prompted the development of numerous spectral vegetation indices (VIs). VIs are dimensionless radiometric measures that combine two or more spectral bands to enhance the vegetative signal, while simultaneously minimizing background effects. Vegetation indices are one of the most widely used remote sensing measurements, and thus, many exist. The most common VIs utilize red and near-infrared canopy reflectances in the form of ratios (e.g. NDVI) or linear combination (e.g. PVI), while others are more complex and also require the derivation of soil correction factors (e.g. MSAVI). Although many indices are well correlated with various plant biophysical parameters, some - such as the NDVI - have received more attention than others.

The Normalized Difference Vegetation Index (NDVI) is a computationally simple index that can be calculated from the red and near infrared data acquired by many satellite systems. The NDVI is calculated as $NDVI = (\rho_{nir} - \rho_{red})/(\rho_{nir} + \rho_{red})$, where ρ_{red} and ρ_{nir} are the reflected radiant fluxes in the red and near-infrared wavelengths, respectively (Rouse et al. 1973). The principle behind the NDVI is based on the relationship between the physiological properties of healthy vegetation and the type and amount of radiation it can absorb and reflect (Gitelson and Kaufman 1998). More specifically,

plant chlorophyll strongly absorbs solar radiation in the red portion of the electromagnetic spectrum, while plant spongy mesophyll strongly reflects solar radiation in the near-infrared region of the spectrum (Jackson and Ezra 1985; Tucker 1979; Tucker et al. 1991). As a result, vigorously growing healthy vegetation has low red-light reflectance and high near-infrared reflectance, and hence, high NDVI values. The NDVI produces output values in the range of -1.0 to 1.0. Increasing positive NDVI values indicate increasing amounts of green vegetation, while NDVI values near zero and decreasing negative values are characteristic of non-vegetated surfaces such as barren surfaces (rock and soil) and water, snow, ice, and clouds (Jensen 2007). It is important to note, however, that because the NDVI becomes less sensitive to plant chlorophyll at high chlorophyll contents, the NDVI approaches saturation asymptotically under moderate-to-high biomass conditions (Baret and Guyot 1991; Gitelson and Kaufman 1998; Huete et al. 2002; Myneni et al. 2002; Sellers 1985). As a result, although the NDVI has been shown to correlate well with many canopy biophysical properties – including vegetation abundance (Hurcom and Harrison 1998; Purevdorj et al. 1998), aboveground biomass (Boutton et al. 1980; Davidson and Csillag 2001; Weiser et al. 1986), green leaf area (Asrar et al. 1986; Baret and Guyot 1991; Weiser et al. 1986), photosynthetically active radiation (PAR) (Asrar et al. 1986; Baret and Guyot 1991; Hatfield et al. 1984; Tucker et al. 1986; Weiser et al. 1986), and productivity (Box et al. 1989; Prince 1991; Running et al. 1989) – it generally does so in a non-linear fashion across low-to-high productivity gradients (Figure 1).

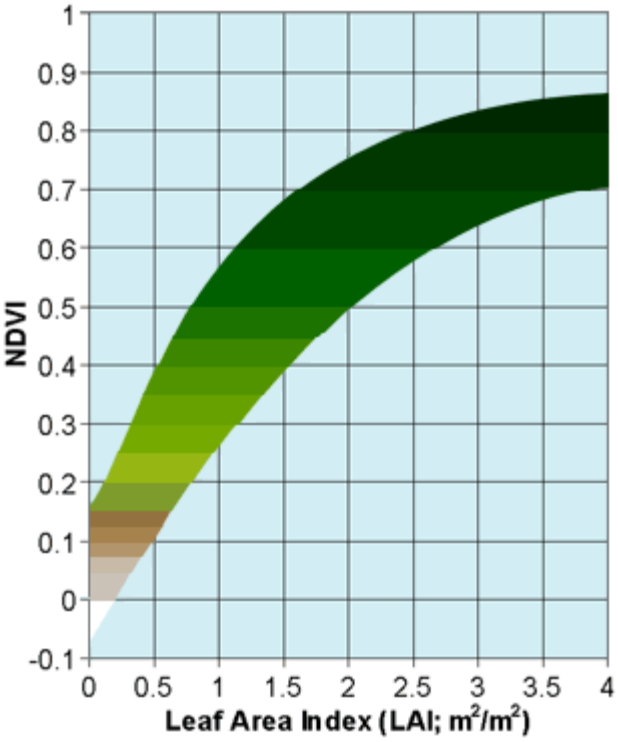

Figure 1. Generalized relationship between NDVI and LAI for a range of soil and vegetation spectral properties (source:

The NDVI has emerged as one of the most robust tools for monitoring natural vegetation and crop conditions. This is largely due to its use in the various NDVI datasets produced from daily reflectance observations collected by the Advanced Very High Resolution Radiometer (AVHRR) instruments flown onboard 14 of NOAA's Polar Orbiting Satellites since 1978. The AVHRR, originally designed for meteorological applications, is a four-channel (AVHRR-1), five-channel (AVHRR-2) or six-channel (AVHRR-3) scanner that senses in the visible, near-infrared, and thermal infrared portions of the electromagnetic spectrum at a spatial resolution of 1.1km (at nadir) (Table 1). The data collected by this series of sensors comprise the longest-lived and most influential series of Earth observing satellites ever launched (Hastings and Emery 1992).

Channel	AVHRR-1: NOAA-6, NOAA-8, NOAA-10	AVHRR-2: NOAA-7, NOAA-9, NOAA-11, NOAA-12, NOAA-14	AVHRR-3: NOAA-15, NOAA-16, NOAA-17, NOAA-18	IFOV (mrad)
1	0.58–0.68	0.58–0.68	0.58–0.68	1.39
2	0.725–1.100	0.725–1.100	0.725–1.100	1.41
3A	—	—	1.59–1.63	1.51
3B	3.55–3.93	3.55–3.93	3.55–3.93	1.51
4	10.50–11.50	10.30–11.30	10.30–11.30	1.41
5	Band 4 repeated	11.50–12.50	11.50–12.50	1.30

Table 1. The range of spectral bands (in µm) for AVHRR-1, -2 and -3 (Latifovic et al. 2005).

	NOAA-16 AVHRR	Terra MODIS
Launch	September 21, 2000 (USA)	December 18, 1999 (USA)
Orbit	843 km	705 km
Swath	2700 km	2330 km (cross track) by 10 km (along track at nadir)
Spectral bands	5 bands	36 bands
Radiometric resolution	10 bits	12 bits
Spatial	1.1 km	250 m (bands 1–2)
resolutions		500 m (bands 3–7)
at nadir		1000 m (bands 8–36)
Repeat coverage	daily	daily
Bandwidth:		
Band 1	0.58–0.68 µm	0.620–0.670 µm
Band 2	0.72–1.0 µm	0.841–0.876 µm
Band 3	A: 1.58–1.64 µm	0.459–0.479 µm
	B: 3.55–3.93 µm	
Band 4	10.3–11.3 µm	0.545–0.565 µm
Band 5	11.5–12.5 µm	1.230–1.250 µm
Band 6		1.628–1.652 µm
Band 7		2.105–2.155 µm

Table 2. Characteristics of AVHRR and MODIS/Terra for remote sensing (Kawamura et al. 2005)

The most commonly-used products derived from the AVHRR are the n-day maximum-value NDVI composites produced by several U.S and Canadian Government agencies (e.g. National Oceanic and Atmospheric Administration (NOAA); National Aeronautics and Space Administration (NASA), Canada Centre for Remote Sensing (CCRS), and Manitoba Remote Sensing Centre (MRSC)) (Cracknell 2001). While the detailed methodologies for creating these datasets vary, maximum-value compositing usually involves (a) examining each NDVI value pixel by pixel for each observation date during the n-day compositing period, (b) determining the maximum-value NDVI for each pixel during the n-day period, and (c) creating a single output image that contains only the maximum NDVI value for each pixel for the n-day period. Maximum-value NDVI compositing has become a popular resource management tool because it captures the dynamics of green-vegetation and minimizes problems common to single-date AVHRR NDVI data, such as those associated with cloud contamination, atmospheric attenuation, surface directional reflectance, and view and illumination geometry (Holben 1986). At present, two Canadian Government Agencies produce maximum-value NDVI composite datasets focusing on a Canadian coverage (National Coverage / 10-day compositing period (CCRS); Prairie Region Coverage / 7-day compositing period (MRSC)).

However, because the AVHRR sensor was not originally designed for monitoring vegetation, it suffers from limitations regarding the design of its red and near infrared channels when formulating

NDVI (Fensholt and Sandholt 2005). Two particularly important limitations of the AVHRR are (a) the overlap of the near infrared channel (0.725 – 1.100µm) with a region of considerable atmospheric water vapour absorption (0.9 to 0.98 µm) that can introduce noise to the remotely sensed signal (Huete et al. 2002; Justice et al. 1991); and (b) the relatively "quick" saturation of the red channel, and hence NDVI, over medium-to-dense vegetation (Gitelson and Kaufman 1998; Huete 1988; Jensen 2007; Myneni et al. 1997). These limitations were directly addressed with the development of a new generation of EO platforms, including the Moderate resolution Imaging Spectroradiometer (MODIS) launched onboard NASA's Terra satellite in December 1999. MODIS, which has been acquiring data in 36 narrow spectral bands since February 2000, was designed to provide data for vegetation and land cover mapping applications. The MODIS sensor offers a number of improvements over the AVHRR for NDVI calculation (Fensholt and Sandholt 2005; Huete et al. 2002; Trishchenko et al. 2002). These include improved (a) spectral resolution; (b) radiometric resolution (c) spatial resolution; (d) geolocation accuracy; and (e) on-board radiometric calibration for producing scaled reflectances (Jensen 2007). The MODIS red and near-infrared channels were selected to avoid the spectral regions of water absorption that constitute a major limitation of the AVHRR (Justice et al. 1991; Vermote and Saleous 2006). Furthermore, the unprecedented radiometric resolution of MODIS Terra makes its red and near-infrared channels more sensitive to small variations in chlorophyll content, thereby lessening how quickly its NDVI saturates over denser vegetation. As a result of these improvements, MODIS Terra holds promise for environmental monitoring in general, and the estimation of vegetation indices in particular (Fensholt and Sandholt 2005).

Crop Condition Assessment using NDVI at AAFC

Severe droughts, increasing competition among grain exporters, and the instability of grain markets have highlighted the importance of having accurate and timely information on crop conditions and potential yield. There is thus a need to produce operational information and applications to help address both the risk of a weather-related disaster occurring and the potential impact of a current weather-related event.

Under normal operational conditions regular monitoring and forecasting will provide a risk assessment of weather–related impact to the agriculture industry and an estimate of the severity of the impact. Providing advanced warning of such impacts will help in planning anticipated mitigation costs and assist the agricultural industry with preparedness. When low- or moderate-level impacts occur, timely information is available to assist the industry in mitigation efforts.

Agriculture and Agri-Food Canada (AAFC) requires regular information on crop conditions across Canada in near-real-time for crop condition assessment purposes. To this end, AAFC has funded Statistics Canada since 2004 to distribute/deliver AVHRR-derived 1km-resolution NDVI composites of the Canadian agriculture extent and the northern half of the United States. These data, available as 7-day national composites are available through the Crop Condition Assessment Program (CCAP), developed and maintained by Statistics Canada since 1987. CCAP is an interactive Web-based

application that monitors changing cropland and pasture conditions during the growing season. These changes in vegetation health are monitored using 1km-resolution digital satellite (AVHRR) data, thematic maps, vegetation index graphs, and tabular data of current and historical cropland and pasture conditions.

However, there are a number of limitations regarding the use of CCAP AVHRR data in AAFC applications. These are (a) the relatively coarse radiometric, spectral and spatial resolutions of the AVHRR's red and near-infrared channels; (b) the non-availability of daily (or n-day) data products; and (c) the restriction of data access to web viewing and web mapping. Limitation (c) is especially important because there is a strong need to have access to the digital products through an Application Programming Interface (API) or web services that are not provided through the Statistics Canada application.

Limitations relating to AVHRR data quality (i.e. radiometric, spectral and spatial resolution) can be directly addressed by using the new generation earth observation platforms, including the Moderate Resolution Imaging Spectroradiometer (MODIS) launched onboard NASA's Terra satellite. MODIS data is available at no cost to the public.

The MODIS Terra sensor offers a number of improvements over the AVHRR for NDVI calculation. These include improved:

(a) spectral resolution;
(b) radiometric resolution (12-bit vs 10-bit for the AVHRR sensor);
(c) spatial resolution (250m for NDVI, compared to 1 km for the AHVRR sensor);
(d) geolocation accuracy;
(e) on-board radiometric calibration for producing scaled reflectances.

In response to the above limitations, AAFC developed an NDVI compositing sub-system (the National Crop Monitoring System Prototype, NCMS-P) that uses data acquired from MODIS to produce weekly / 7-day (or n-day) Max-NDVI composites for Canada south of 60°N. As of 2009, AAFC has provided open access to these data, either indirectly though the previously-described CCAP web mapping application hosted by Statistics Canada, or directly through an AAFC ftp site.

A National Crop Monitoring System Prototype (NCMS-P)

1.3.1 The NCMS-P Toolset

AAFC has developed a set of individual tools for generating weekly Max-NDVI composites and their associated weekly Max-NDVI anomalies (differences from the n-year average Max-NDVI conditions for that week). These tools use MODIS Level-2 Gridded (L-2G) surface reflectance data (collection V005).

Six tools are used to create weekly Max-NDVI composites, weekly average Max-NDVI baselines and weekly Max-NDVI anomalies in near-real-time from these MODIS data. The tools carry out the following tasks:

(a) Download of MODIS HDF data tiles (granules) from USGS Data Archive;
(b) Extraction of required science datasets (as TIF format) from HDF tiles;

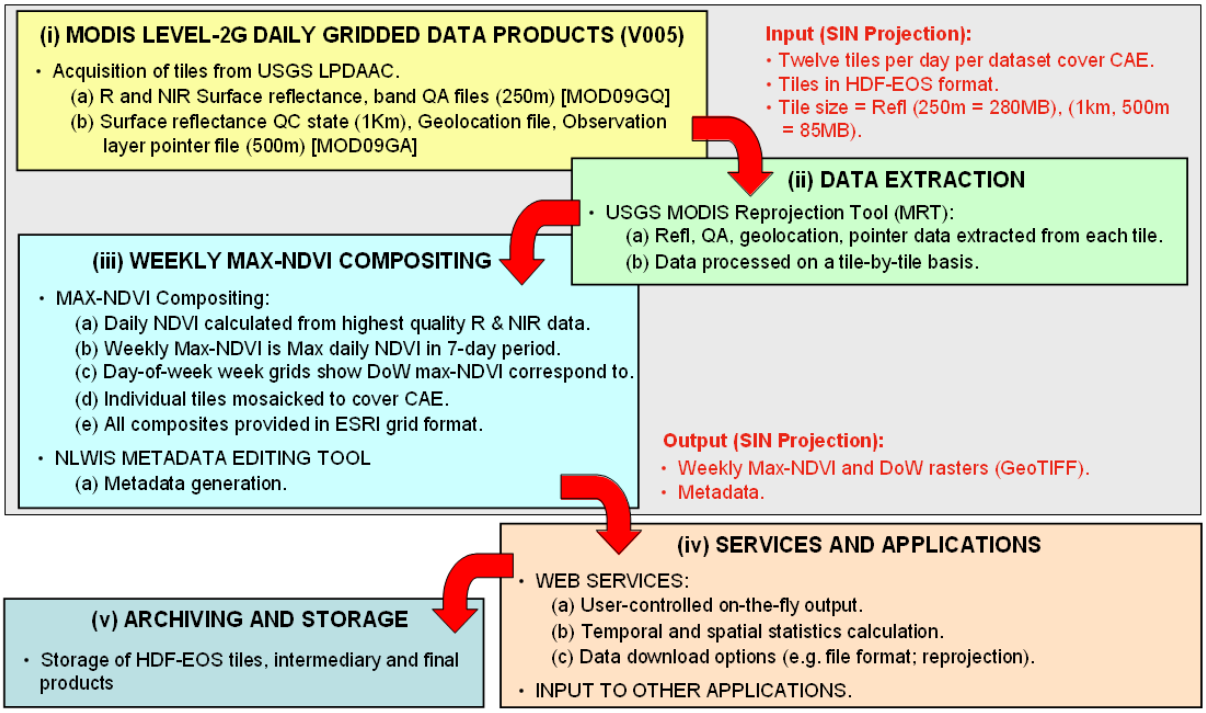

(c) Check for missing TIF files and gap filling if tiles are unavailable on USGS archive;
(d) Generation of weekly Max-NDVI and associated Day-of-Week composites;
(e) Generation of weekly historical (n-year) NDVI average baselines (2000-current year); and
(f) Generation of weekly Max-NDVI anomalies.

These scripts use the *ArcGIS Geoprocessor Object*, an object that that provides a single access point and environment for the execution of any geoprocessing tool in ArcGIS V9.3, including extensions. Scripts are coded using Python 2.5. AAFC is presently updating NCMS-P to take advantage of recent Departmental software upgrades to ArcGIS V10.0 and Python 2.6. Initial tests suggest that these upgrades will speed up the time taken to create the above MODIS-related products by 15-25%.

Note that although the primary output products of our near-real-time processing are generated for weekly (7-day) time periods, NCMS-P can be used to generated Max-NDVI-related composites for any n-day period.

Figure 2a, illustrates the steps involved in generating weekly Max-NDVI composites in near-real-time. These steps are discussed in further detail in the following sections.

1.3.2 Required MODIS Datasets

NCMS-P uses two MODIS/Terra daily Level-2G MODIS/Terra products (V005):

(a) Surface Reflectance Daily L2G Global 250m SIN Grid V005 [MOD09GQ].
(b) Surface Reflectance Daily L2G Global 1km and 500m SIN Grid V005 [MOD09GA].

Data for each of the above products are stored in NASA's Land Processes Distributed Active Archive Center (LP DAAC) as tiles (granules) in HDF-EOS format (Hierarchical Data Format; *.hdf). Each tile covers an area of approximately 10º by 10º and is in an integrated sinusoidal (ISIN) projection using the WGS84 datum. Twelve tiles are required to completely cover Canada's landmass south of 60ºN latitude for any single day. A weekly Max-NDVI composite thus uses 7 days *12 tiles = 84 tiles for each of the MOD09GQ and MOD09GA products (168 tiles in total). The ISIN-projected tiles used to cover Canada south of 60ºN latitude are shown in Figure 3.

Each tile contains >1 science dataset (SD). A single tile for the MOD09GQ product contains 5 SDs. A single tile for the MOD09GA product contains 21 SDs. NCMS-P uses 7 SDs in total for each day of the compositing period (three SDs from MOD09GQ and four SDs from MOD09QA). A weekly Max-NDVI composite thus uses 7 days *12 tiles * 7 SDs = 588 SDs. SDs are extracted from the HDF-EOS source files using the MODIS Reprojection Tool. The extraction process converts SDs from the HDF-EOS file format to the GeoTIFF file format (note that the native ISIN projection of the *.hdf tiles is retained).

The SDs contained in the MOD09GQ and MOD09GA products are outlined in Figures 4a and b and 5a, b, and c, below.

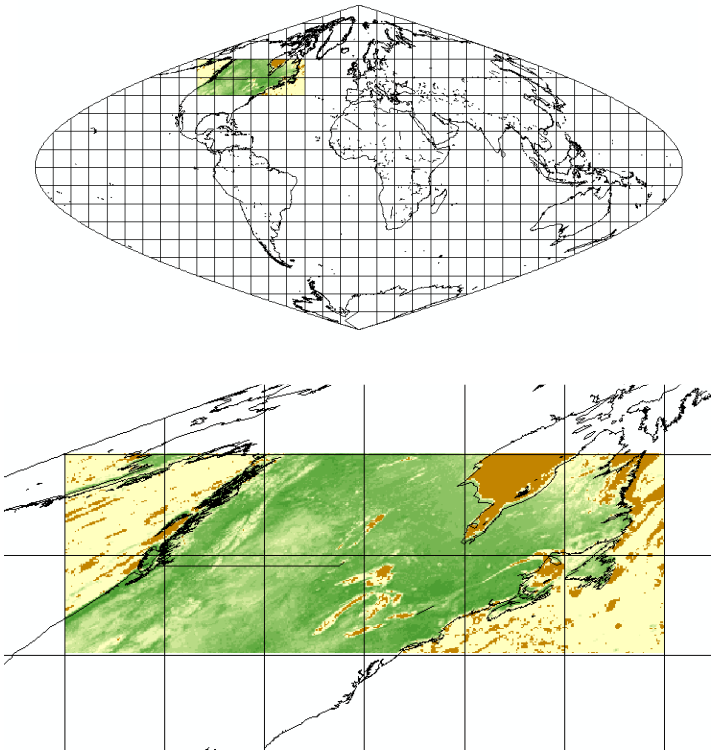

Figure 3: MODIS Integrated Sinusoidal (ISIN) native projection

Science Data Sets (HDF Layers) (5)	UNITS	BIT TYPE	FILL	VALID RANGE	MULTIPLY BY SCALE FACTOR
num_observations: number of observations within the pixel	None	8-bit signed integer	-1	0–127	na
250m Surface Reflectance Band 1 (620-670 nm)	Reflectance	16-bit signed integer	-28672	-100–16000	0.0001
250m Surface Reflectance Band 2 (841-876 nm)	Reflectance	16-bit signed integer	-28672	-100–16000	0.0001
250m Reflectance Band Quality	Bit Field	16-bit unsigned integer	2995	0–4096	na
obs_cov: percentage of the grid cell area is covered by the observation	Percent	8-bit signed integer	-1	0–100	(0.001) 0.009999999776482582

Figure 4a: Science Data Sets for MODIS Terra Surface Reflectance Daily L2G Global 250m SIN Grid V005 (MOD09GQ). Red arrows indicate the science datasets used in the NCMS-P process. Note that the 250m reflectance band quality SD is a bit field, where the values of sequences of bits (rather than the actual pixel value) describe the quality of the product (see Figure 4b).

Bit No.	Parameter Name	Bit Comb.	Sur_refl_qc_250m
0–1	MODLAND QA bits	00	corrected product produced at ideal quality all bands
		01	corrected product produced at less than ideal quality some or all bands
		10	corrected product not produced due to cloud effects all bands
		11	corrected product not produced due to other reasons some or all bands may be fill value [Note that a value of (11) overrides a value of (01)].
2–3	cloud state	00	clear
		01	cloudy
		10	mixed
		11	not set; assumed clear
4–7	band 1 data quality four bit range	0000	highest quality
		1000	dead detector; data interpolated in L1B
		1001	solar zenith >= 86 degrees
		1010	solar zenith >= 85 and < 86 degrees
		1011	missing input
		1100	internal constant used in place of climatological data for at least one atmospheric constant
		1101	correction out of bounds, pixel constrained to extreme allowable value
		1110	L1B data faulty
		1111	not processed due to deep ocean or clouds
8–11	band 2 data quality four bit range		SAME AS BAND ABOVE
12	atmospheric correction performed	1	yes
		0	no
13	adjacency correction performed	1	yes
		0	No
14–15	spare (unused)	-	---

Figure 4b: MOD09GQ.005 250-meter Surface Reflectance Data QA Descriptions (16-bit). Green arrows indicate the bit combinations used in the NCMS-P quality control process.

DATA GROUP	Science Data Sets (HDF Layers) (9)	UNITS	BIT TYPE	FILL	VALID RANGE	MULTIPLY BY SCALE FACTOR
1km (1)	num_observations_1km: Number of Observations	na	8-bit signed integer	-1	0–127	na
	State_1km: Reflectance Data State QA	Bit Field	16-bit unsigned integer	65535	0–57335	na
	SensorZenith	Degree	16-bit signed integer	-32767	0–18000	0.01
	SensorAzimuth	Degree	16-bit signed integer	-32767	-18000–18000	0.01
	Range: pixel to sensor	Meter	16-bit unsigned integer	65535	27000–65535	25
	SolarZenith	Degree	16-bit signed integer	-32767	0–18000	0.01
	SolarAzimuth	Degree	16-bit signed integer	-32767	-18000–18000	0.01
	gflags: Geolocation flags	Bit Field	8-bit unsigned integer	255	0–248	na
	orbit_pnt: Orbit pointer	none	8-bit signed integer	-1	0–15	na

Figure 5a: Science Data sets for MODIS Terra Surface Reflectance Daily L2G Global 1km and 500m SIN Grid V005 (MOD09GA). Red arrows indicate the science datasets used in the NCMS-P process. Note that the 1km reflectance state QA SD is a bit field, where the values of sequences of bits (rather than the actual pixel value) describe the quality of the product.

[Table continued on next page…]

DATA GROUP	Science Data Sets (HDF Layers) (12)	UNITS	BIT TYPE	FILL	VALID RANGE	MULTIPLY BY SCALE FACTOR
500m (2)	num_observations_500m	none	8-bit signed integer	-1	0–127	na
	sur_refl_b01: 500m Surface Reflectance Band 1 (620-670 nm)	Reflectance	16-bit signed integer	-28672	-100–16000	0.0001
	sur_refl_b02: 500m Surface Reflectance Band 2 (841-876 nm)	Reflectance	16-bit signed integer	-28672	-100–16000	0.0001
	sur_refl_b03: 500m Surface Reflectance Band 3 (459-479 nm)	Reflectance	16-bit signed integer	-28672	-100–16000	0.0001
	sur_refl_b04: 500m Surface Reflectance Band 4 (545-565 nm)	Reflectance	16-bit signed integer	-28672	-100–16000	0.0001
	sur_refl_b05: 500m Surface Reflectance Band 5 (1230-1250 nm)	Reflectance	16-bit signed integer	-28672	-100–16000	0.0001
	sur_refl_b06: 500m Surface Reflectance Band 6 (1628-1652 nm)	Reflectance	16-bit signed integer	-28672	-100–16000	0.0001
	sur_refl_b07: 500m Surface Reflectance Band 7 (2105-2155 nm)	Reflectance	16-bit signed integer	-28672	-100–16000	0.0001
	QC_500m: 500m Reflectance Band Quality	Bit Field	32-bit unsigned integer	787410671	0–4294966019	na
	Obs_cov_500m: Observation coverage	Percent	8-bit signed integer	-1	0–100	(0.01) 0.00999999977648258
	iobs_res: Observation number	none	8-bit unsigned integer	255	0–254	na
	q_scan: 250m scan value information	Bit Field	8-bit unsigned integer	255	0–255	na

Figure 5a (Continued): Science Data sets for MODIS Terra Surface Reflectance Daily L2G Global 1km and 500m SIN Grid V005 (MOD09GA). Red arrows indicate the science datasets used in the NCMS–P process.

Bit No.	Parameter Name	Bit Comb.	state_1km
0–1	cloud state	00	clear
		01	cloudy
		10	mixed
		11	not set, assumed clear
2	cloud shadow	1	yes
		0	no
3–5	land/water flag	000	shallow ocean
		001	land
		010	ocean coastlines and lake shorelines
		011	shallow inland water
		100	ephemeral water
		101	deep inland water
		110	continental/moderate ocean
		111	deep ocean
6–7	aerosol quantity	00	climatology
		01	low
		10	average
		11	high
8–9	cirrus detected	00	none
		01	small
		10	average
		11	high
10	internal cloud algorithm flag	1	cloud
		0	no cloud
11	internal fire algorithm flag	1	fire
		0	no fire
12	MOD35 snow/ice flag	1	yes
		0	no
13	Pixel is adjacent to cloud	1	yes
		0	no
14	BRDF correction performed	1	yes
		0	no
15	internal snow mask	1	snow
		0	no snow

Figure 5b: MOD09GA 1-kilometer State QA Descriptions (16-bit). Green arrows indicate the bit combinations used in the NCMS-P quality control process.

Bit No.	Parameter Name	Bit Comb.	q_scan
0	missing observation in quadrant 4 [+0.5 row, +0.5 column]	1	yes
		0	no
1	missing observation in quadrant 3 [+0.5 row, -0.5 column]	1	yes
		0	no
2	missing observation in quadrant 2 [-0.5 row, +0.5 column]	1	yes
		0	no
3	missing observation in quadrant 1 [-0.5 row, -0.5 column]	1	yes
		0	no
4	scan of observation in quadrant 4 [+0.5 row, +0.5 column]	1	same
		0	different
5	scan of observation in quadrant 3 [+0.5 row, +0.5 column]	1	same
		0	different
6	scan of observation in quadrant 2 [+0.5 row, +0.5 column]	1	same
		0	different
7	scan of observation in quadrant 1 [+0.5 row, +0.5 column]	1	same
		0	different

Figure 5c: 250-meter Scan Value Information Description (8-bit)

The necessary SDs are extracted from the downloaded *.hdf tiles using the MODIS Reprojection Tool software.

1.3.3 Generating Max-NDVI Composites Using Best Quality Data

Once SD extraction is complete, the Max-NDVI compositing algorithm is implemented. This algorithm uses Band 1 and Band 2 surface reflectance at 250m resolution, along with the QA flags, to produce an n-day Max-NDVI composite from only the “best quality” reflectance retrievals. The general concept is to retain pixels in the Max-NDVI procedure that are (i) not influence by atmospheric effects, and (ii) fall within the range of acceptable sensor and sun illumination angles.

Specifically, screening involves the elimination of pixels that are contaminated by clouds, cloud shadow, high amounts of aerosols, and high amounts of cirrus. In addition, pixels collected at unacceptable

viewing and sun illumination angles are also eliminated. The screening rules for the selection of acceptable retrievals are summarized in Figure 6.

Data Product	Science Dataset	Bits (if bit field)	Quality Criteria	Bitmap Value
MOD09GQ	250m Reflectance Band Quality	0-1	MODLAND QA = Corrected product at ideal quality all bands	== 0
		2-3	Cloud state = clear	== 0
		4-7	Band 1 data quality = highest quality	== 0
		8-11	Band 2 data quality = highest quality	== 0
MOD09GA	State_1km: Reflectance Data State QA	2	Cloud shadow = no	== 0
		6-7	Aerosol quantity = not high	<> 3
		8-9	Cirrus quantity = not high	<> 3
	Sensor Zenith	-	Sensor zenith between 0 and 45 degrees	>= 0 and <= 4500

Figure 6: Pixel screening criteria used to generate MODIS Max-NDVI composites of high quality.

1.3.3.Gap-Filling Missing Data

In some cases, not all *.hdf tiles are available for a given week. This is problematic because the current version of NCMS-P does not handle missing data files. To address this problem, data gaps are “filled”. Filling gaps involves (a) identifying the GeoTIFF files expected for an n-day, n-tile composite (usually, 7-day, 12-tiled), (b) identifying if any of the expected tiles are missing, and (c) using the available tiles to fill gaps in the data (missing hdf files for a given day are gap-filled using the hdf files extracted for the previous or subsequent day. Note that if any SDs are missing for a given day – even just one of the 7 required for input to NCMS – all 7 SDs for are replaced in the gap-filling process).

1.3.4. Output Products: Max-NDVI and Day-of-Week Composites

The compositing tool generates four outputs. These are: (i) a Max-NDVI composite for the 7-day 12-tile compositing period, where NDVI ranges from -1 to 1 (nmcom*); (ii) a rescaled version of this NDVI composite, where negative NDVI values (NDVI < 0) are set to 0 (rncom*); and (iii) a day-of-week (DOW) composite where pixel values correspond to the day of the compositing period from which their Max-NDVI value is taken (dow*). Rescaled Max-NDVI composites are created to separate the NDVI range that is typical of vegetation canopies from the NDVI range typical of other surfaces (NDVI produces output values in the range of -1.0 to 1.0. Increasing positive NDVI values indicate increasing amounts of green vegetation, while NDVI values near zero and decreasing negative values are characteristic of non-vegetated surfaces such as rock, soil, water, snow, ice, and clouds (Jensen 2007).

Figures 7 and 8 illustrate output rasters generated by the compositing tool. The example shown here uses 12 tiles of MODIS data for a 7-day period (DOY 117-123, 2009). NDVI composites are generated as 32-bit float Geotiff rasters. DOW composites are generated as 8-bit Geotiff rasters. All GeoTiff rasters remain in their native sinusoidal projection (Fig. 8).

C:\MODPROC\DEMO\TMP

Name	Size	Modified
dow2009117to123.aux	11,866	2009-05-15 1:33:44 AM
dow2009117to123.rrd	10,460,388	2009-05-15 1:33:44 AM
dow2009117to123.tif	277,561,736	2009-05-15 1:33:18 AM
dow2009117to123.tif.vat.dbf	231	2009-05-15 1:33:32 AM
dow2009117to123.tif.xml	1,624	2009-05-15 1:33:44 AM
ncom2009117to123.aux	534,761	2009-05-15 1:26:23 AM
ncom2009117to123.rrd	92,874,178	2009-05-15 1:26:23 AM
ncom2009117to123.tif	1,107,001,736	2009-05-15 1:25:20 AM
ncom2009117to123.tif.xml	1,602	2009-05-15 1:26:24 AM
rncom2009117to123.aux	534,930	2009-05-15 1:38:36 AM
rncom2009117to123.rrd	84,806,152	2009-05-15 1:38:35 AM
rncom2009117to123.tif	1,107,541,652	2009-05-15 1:38:35 AM
rncom2009117to123.tif.xml	953	2009-05-15 1:38:37 AM

Figure 7: Directory listing showing GeoTiff rasters generated by the n-day Max-NDVI compositing tool (example shown is a 7-day period from day-of-year 117 to 123, 2009, using 12 tiles).

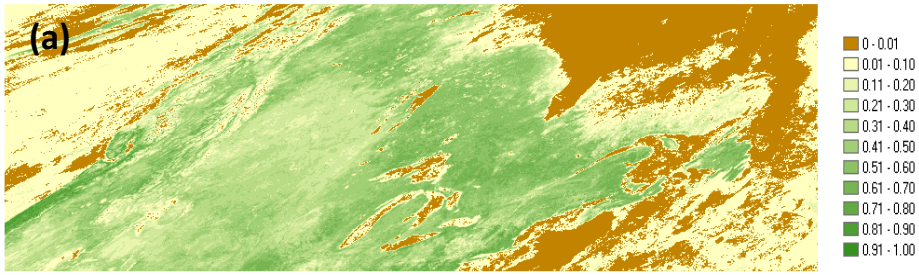

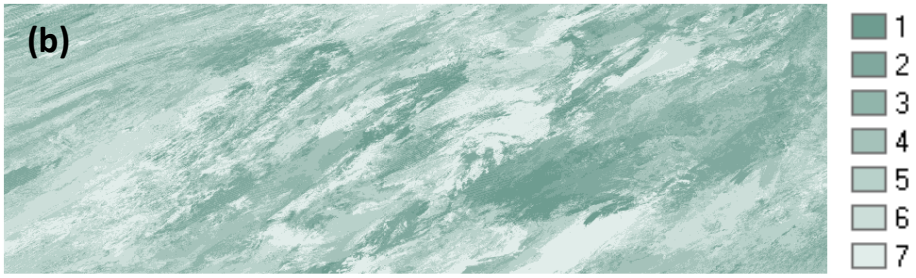

Figure 8: (a) Re-scaled Maximum NDVI composite (where NDVI ranges from 0-1), and (b) Day-of-week (DOW) composite, where pixel values are assigned the value corresponding to the day of the compositing period from which their Max-NDVI value is taken. Note that composites remain in their native sinusoidal projection.

1.3.5. Output Products: Output Products: Baseline and Standard Deviation composites

The generation of weekly Max-NDVI and DOW is not the end of the processing chain. We are often interested in how the current week's NDVI compares to the "historical" average (baseline) Max-NDVI conditions for that week. To do this, we must calculate the mean NDVI conditions for the week in question across the entire MODIS historical record, then calculate the difference (anomaly) between the current week's Max-NDVI (current conditions) and the baseline.

The baseline calculation tool generates two outputs. These are: (i) a baseline Max-NDVI composite for each week in the growing season (used to describe the long term "baseline" Max-NDVI conditions for a given week) (Av.MaxNDVI.*); and (ii) a standard-deviation Max-NDVI composite for each week in the growing season (used to describe the historical variability in Max-NDVI values for a given week) (St.MaxNDVI.*).

Figures 10 and 11 illustrate output rasters generated by the baseline calculation tool. The example shown here uses 12 tiles of MODIS data for week 18 2000-2009. Baseline and standard deviation composites are generated as 32-bit float Geotiff rasters. All GeoTiff rasters remain in their native sinusoidal projection (Fig. 11).

C:\MODPROC\B\W18.Base

Name	Size	Modified
Av.MaxNDVI.2000.2009.Week.18.aux	534,966	2009-05-15 7:38:28 AM
Av.MaxNDVI.2000.2009.Week.18.rrd	90,764,078	2009-05-15 7:38:27 AM
Av.MaxNDVI.2000.2009.Week.18.tif	1,107,541,652	2009-05-15 7:38:27 AM
Av.MaxNDVI.2000.2009.Week.18.tif.xml	1,288	2009-05-15 7:38:28 AM
Logfile.AvStdv.MaxNDVI.2000.2009.Week.18.txt	800	2009-05-15 8:03:33 AM
St.MaxNDVI.2000.2009.Week.18.aux	534,966	2009-05-15 8:03:31 AM
St.MaxNDVI.2000.2009.Week.18.rrd	90,764,088	2009-05-15 8:03:29 AM
St.MaxNDVI.2000.2009.Week.18.tif	1,107,541,652	2009-05-15 8:03:29 AM
St.MaxNDVI.2000.2009.Week.18.tif.xml	1,287	2009-05-15 8:03:31 AM

Figure 10: Directory listing showing GeoTiff rasters generated by the baseline calculation tool: Averages (Av.MaxNDVI.) and standard deviation (St.MaxNDVI.*) (example shown for week 18, 2000-2009). Note also the logfile that contains information on the files used as input to the calculations.*

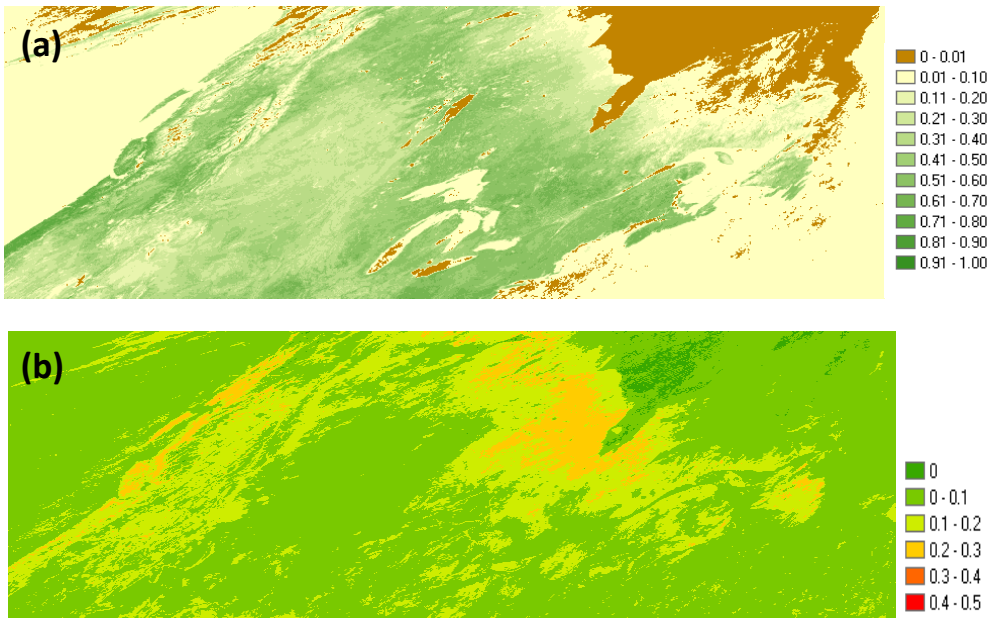

Figure 11: (a) The baseline (mean) of Max-NDVI for week 18 (2000-2009) and (b) the standard deviation of Max-NDVI for week 18 (2000-2009). We use the rescaled Max-NDVI composites (rncom; NDVI ranges from 0-1) in the baseline and standard deviation calculations. Note that composites remain in their native sinusoidal projection.*

1.3.6: Output Product: Anomaly composites

The compositing tool generates one output: anomaly composite for each weekly Max-NDVI composite (note: baselines and anomalies are calculated using the rescaled Max-NDVI products).

Figures 13 and 14 illustrate output rasters generated by the anomaly calculation tool. The example shown uses the Max-NDVI composite for week 18 2009 (DOY 117-123, 2009) and the baseline created for week 18 using the ten weekly composites for week 18 from 2000-2009. Anomaly composites are generated as 32-bit float Geotiff rasters. All GeoTiff rasters remain in their native sinusoidal projection (Fig. 14).

C:\MODPROC\B\W18.Anom

Name	Size	Modified
Anom2009117to123.Week.18.aux	534,966	2009-05-15 8:14:00 AM
Anom2009117to123.Week.18.rrd	90,764,074	2009-05-15 8:13:59 AM
Anom2009117to123.Week.18.tif	1,107,541,652	2009-05-15 8:13:59 AM
Anom2009117to123.Week.18.tif.xml	943	2009-05-15 8:14:00 AM

Figure 13: Directory listing showing GeoTiff rasters generated by the calculation tool (example shown for difference between week 18 2009 and the baseline calculated by week 18 Max-NDVI composites for the years 2000-2009).

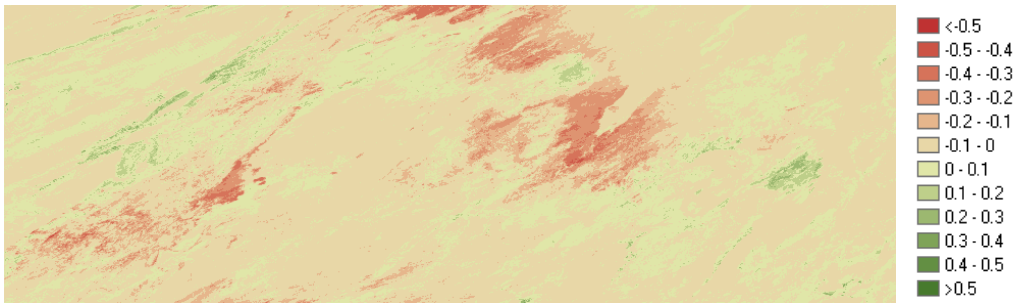

Figure 14: The NDVI anomaly for week 18 2009. This anomaly is calculated as the difference in NDVI between the Max-NDVI composite for this week and the ten-year average (baseline) NDVI for this week. Note that composites remain in their native sinusoidal projection.

References

Asner, G.P. (1998). Biophysical and biochemical sources of variability in canopy reflectance. *Remote Sensing of Environment, 64*, 234-253

Asner, G.P., Wessman, C.A., Schimel, D.S., & Archer, S. (1998). Variability in leaf and litter optical properties: implications for BRDF model inversions using AVHRR, MODIS and MISR. *Remote Sensing of Environment, 63*, 243-257

Asrar, G., Weiser, R.L., Johnson, D.E., Kanemasu, E.T., & Milleen, J.M. (1986). Distinguishing among tallgrass prairie cover types from measurements of multispectral reflectance. *Remote Sensing of Environment, 19*, 159-169

Bakhtiari, & Zoughi (1991). A model for backscattering characteristics of tall prairie grass canopies at microwave frequencies. *Remote Sensing of Environment, NA*, 137-147

Baret, F., & Guyot, G. (1991). Potentials and limits of vegetation indices for LAI and APAR assessment. *Remote Sensing of Environment, 35*, 161-173

Boutton, T.W., Harrison, A.T., & Smith, B.N. (1980). Distribution of biomass of species differing in photosynthetic pathway along an altitudinal gradient in southeastern Wyoming grassand. *Oecologia, 45*, 287-298

Box, E.O., Holben, B.N., & Kalb, H. (1989). Accuracy of the AVHRR vegetation index as a predictor of biomass, primary productivity and net CO2 flux. *Vegetatio, 80*, 71-89

Cracknell, A.P. (2001). The exciting and titally unanticipated asuccess of the AVHRR in applications for which it was never intended. *Advances in Space Research, 28*, 233-240

Davidson, A., & Csillag, F. (2001). The influence of vegetation index and spatial resolution on a two-

date remote sensing derived relation to C4 species coverage. *Remote Sensing of Environment, 75*, 138-151

Fensholt, R., & Sandholt, I. (2005). Evaluation of MODIS and NOAA AVHRR vegetation indices with in situ measurements in a semi-arid environment. *International Journal of Remote Sensing, 26*, 2561-2594

Fourty, T., Baret, F., Jacquemoud, S., Schmuck, G., & Verdebout, J. (1996). Leaf optical properties with explicit description of its biochemical composition: direct and inverse problems. *Remote Sensing of Environment, 56*, 104-117

Gitelson, A.A., & Kaufman, Y.J. (1998). MODIS NDVI Optimization To Fit the AVHRR Data Series--Spectral Considerations. *Remote Sensing of Environment, 66*, 343-350

Goel, N.S. (1988). Models of vegetation canopy reflectance and their use in estimation of biophysical parameters from reflectance data. *Remote Sensing of Environment, 4*, 1-212

Hastings, D.A., & Emery, W.J. (1992). The Advanced Very High Resolution Radiometer (AVHRR): A Brief Reference Guide. *Photogrammetric Engineering and Remote Sensing, 58*, 1183-1188

Hatfield, J.L., Asrar, G., & Kanemasu, E.T. (1984). Intercepted photosynthetically active radiation estimated by spectral reflectance. *Remote Sensing of Environment, 14*, 65-75

Holben, B. (1986). Characteristics of maximum value composite images from temporal AVHRR data. *International Journal of Remote Sensing, 7*, 1417-1434

Huete, A., Didan, K., Miura, T., Rodriguez, E.P., Gao, X., & Ferreira, L.G. (2002). Overview of the radiometric and biophysical performance of the MODIS vegetation indices. *Remote Sensing of Environment, 83*, 195-213

Huete, A.R. (1988). A soil-adjusted vegetation index (SAVI). *Remote Sensing of Environment, 25*, 295-309

Hurcom, S.J., & Harrison, A.R. (1998). The NDVI and spectral decomposition for semi-arid vegetation abundance estimation. *International Journal of Remote Sensing, 19*, 3109-3125

Jackson, T.J., & Ezra, C.E. (1985). Spectral response of cotton to suddenly induced water stress. *International Journal of Biometeorology, 6*, 177-185

Jensen, J.R. (2007). *Remote Sensing of the Environment: An Earth Resource Perspective*. Upper Saddle River, NJ, USA: Prentice Hall

Justice, C.O., Eck, T.F., Tanr, eacute, D., & Holben, B.N. (1991). The effect of water vapour on the normalized difference vegetation index derived for the Sahelian region from NOAA AVHRR data. *International Journal of Remote Sensing, 12*, 1165 - 1187

Kawamura, K., Akiyama, T., Yokota, H.-o., Tsutsumi, M., Yasuda, T., Watanabe, O., & Wang, S. (2005). Comparing MODIS vegetation indices with AVHRR NDVI for monitoring the forage quantity and quality in Inner Mongolia grassland, China. *Grassland Science, 51*, 33-40

Latifovic, R., Trishchenko, A.P., Chen, J., Park, W.B., Khlopenkov, K.V., Fernandes, R., Pouliot, D., Ungureanu, C., Luo, Y., Wang, S., Davidson, A., & Cihlar, J. (2005). Generating historical AVHRR 1 km baseline satellite data records over Canada suitable for climate change studies. *Canadian Journal of Remote Sensing, 31*, 324-346

Myeni, R.B., Ross, J., & Asrar, G. (1989). A review on the theory of photon transport in leaf canopies. *Agricultural and Forest Meteorology, 45*, 1-153

Myneni, R.B., Hoffman, S., Knyazikhin, Y., Privette, J.L., Glassy, J., Tian, Y., Wang, Y., Song, X., Zhang,

Y., & Smith, G.R. (2002). Global products of vegetation leaf area and fraction absorbed PAR from year one of MODIS data. *Remote Sensing of Environment, 83*, 214-231

Myneni, R.B., Ramakrishna, R., Nemani, R.R., & Running, S.W. (1997). Estimation of global leaf area index and absrobed PAR using radiative transfer models. *IEEE Transactions on Geoscience and Remote Sensing, 35*, 1380-1393

Prince (1991). A model of regional primary production for use with coarse resolution satellite data. *International Journal of Remote Sensing, 6*, 1313-1330

Purevdorj, T., Tateishi, R., Ishiyama, T., & Honda, Y. (1998). Relationships between percent vegetation cover and vegetation indices. *International Journal of Remote Sensing, 19*, 3519-3535

Ross, J.K. (1981). *The radiation regime and architecture of plant stands*. Hingham, MA, USA: Kluwer Boston

Rouse, J.W., Haas, R.H., Schell, J.A., & Deering, D.W. (1973). Monitoring vegetation systems in the Great Plains with ERTS-1. In (pp. 309-317)

Running, S.W., Nemani, R.R., Peterson, D.L., Band, L.E., Potts, D.F., Pierce, L.L., & Spanner, M.A. (1989). Mapping regional evapotranspiration and photosynthesis by coupling satellite data with ecosystem simulation. *Ecology, 70*, 1090-1101

Sellers, P.J. (1985). Canopy reflectance, photosynthesis and transpiration. *International Journal of Remote Sensing, 6*, 1335-1372

Trishchenko, A.P., Cihlar, J., & Li, Z. (2002). Effects of spectral response function on surface reflectance and NDVI measured with moderate resolution satellite sensors. *Remote Sensing of Environment, 81*, 1-18

Tucker, C.J. (1979). Red and photographic infrared linear combinations for monitoring vegetation. *Remote Sensing of Environment, 8*, 127-150

Tucker, C.J. (1980). Remote sensing of leaf water content in the near infrared. *Remote Sensing of Environment, 10*, 23-32

Tucker, C.J., Fung, I.Y., Keeling, C.D., & Gammon, R.H. (1986). Relationship between atmospheric CO2 variations and satellite-derived vegetation index. *Nature, 319*, 195–199

Tucker, C.J., Newcomb, W.W., Los, S.O., & Prince, S.D. (1991). Mean and inter-year variation of growing-season normalized difference vegetation index for the Sahel 1981-1989. *International Journal of Remote Sensing, 12*, 1133-1135

Vermote, E.F., & Saleous, N.Z. (2006). Calibration of NOAA16 AVHRR over a desert site using MODIS data. *Remote Sensing of Environment, 105*, 214-220

Weiser, R.L., Asrar, G., Miller, G.P., & Kanemasu, E.T. (1986). Assessing grassland biophysical characteristics from spectral measurements. *Remote Sensing of Environment, 20*, 141-152